Electronic Supplementary Material (ESI) for Journal of Materials Chemistry A.
This journal is © The Royal Society of Chemistry 2019

Supporting Information for:

Water oxidation catalysis on reconstructed $NaTaO_3$ (001) surfaces

Hassan Ouhbi and Ulrich Aschauer
Department of Chemistry and Biochemistry, University of Bern, Freiestrasse 3, CH-3012 Bern, Switzerland
(Dated: June 13, 2019)

S1. CONVERGENCE TESTS

Surface energies, O* adsorption energies and band gaps for slabs with 2, 3 and 4 unit-cell layers thickness are shown in Table S1. While differences in surface energy, O* adsorption energy and band gap between the 2 and 3 unit-cell layer thick slabs are still significant, they become of the order of the DFT error when comparing the 3 and 4 unit-cell layer thick slabs. The same is true for the electronic structure as shown by the DOS in Fig. S1.

Table S1. Convergence of the surface energy, O* adsorption energy and band gap of the terraced reconstructed (001) surface with thickness of 2, 3 and 4 unit cell layers.

Unit-cell layers	Surface energy (J/m^2)	*O adsorption energy (eV)	Band gap (eV)
2	1.23	1.83	1.49
3	1.21	1.67	1.34
4	1.20	1.68	1.30

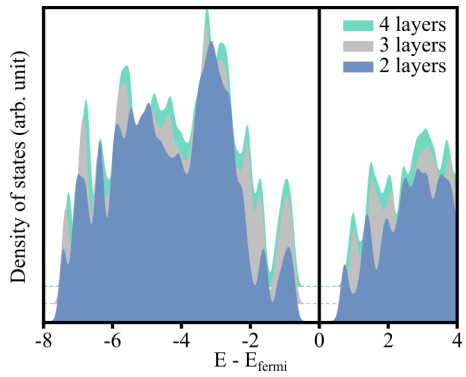

Figure S1. Density of states as a function of the slab thickness for the reconstructed (001) surface. The baselines have been offset vertically for clarity.

The electrostatic potential along the surface normal direction is shown in Fig. S2. The vacuum thickness of 15Å combined with the dipole correction leads to a flat electrostatic potential in the vacuum region.

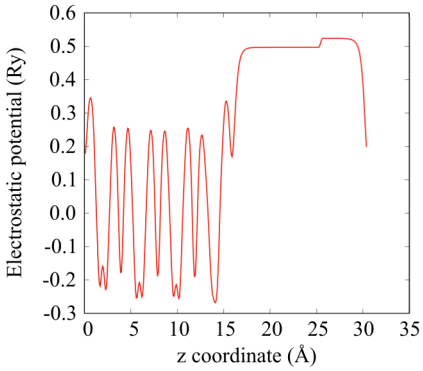

Figure S2. Plane-averaged electrostatic potential of the reconstructed (001) surface

S2. BINDING GEOMETRY

In Figure S3 we show the adsorption geometry of the OOH adsorbate at the Ta_1 site close to the step edge and the Ta_2 site further from the step edge of the clean reconstructed $NaTaO_3$ (001) surface. For the O and OH adsorbates we do not see significant changes in geometry and do hence not present them here. We observe close to the step a longer hydrogen bond, while the Ta-O bond is very similar at both sites. From the shorter H-bond, we would thus expect a stronger binding of the adsorbate at the Ta_2 site, which is however opposed to the binding energy data reported in the main text. We thus conclude that the difference in binding energy between Ta_1 and Ta_2 sites does not stem from the different geometry and H-bonds of the adsorbates but most likely from their interaction with the step edge and the Na atoms in particular.

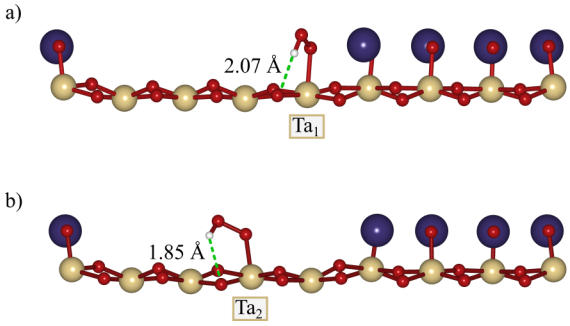

Figure S3. Adsorption geometry of OOH on a) the Ta_1 site and b) the Ta_2 site of the clean reconstructed $NaTaO_3$ (001) surface. The dashed green line shows the hydrogen bond length.

S3. FREE ENERGY DIAGRAMS

Figure S4 shows the computed OER free energy profile under operating conditions considering the conventional, coupling and lattice-oxygen mechanisms at different sites. We see that step B (O formation) is the ODS for all Ta sites, while sites at the step edge have a lower overpotential of 1.11 V. For the coupling mechanism both pathways have step C' (deprotonation of the first OH) as the ODS and the pair close to the step edge (C_1) has a lower overpotential. For the lattice mechanism on the NaO terrace finally, both sites have step D (deprotonation of OH at the LO site) as the ODS, however with very different overpotentials and a largely higher activity for the LO_1 site at the center of the terrace.

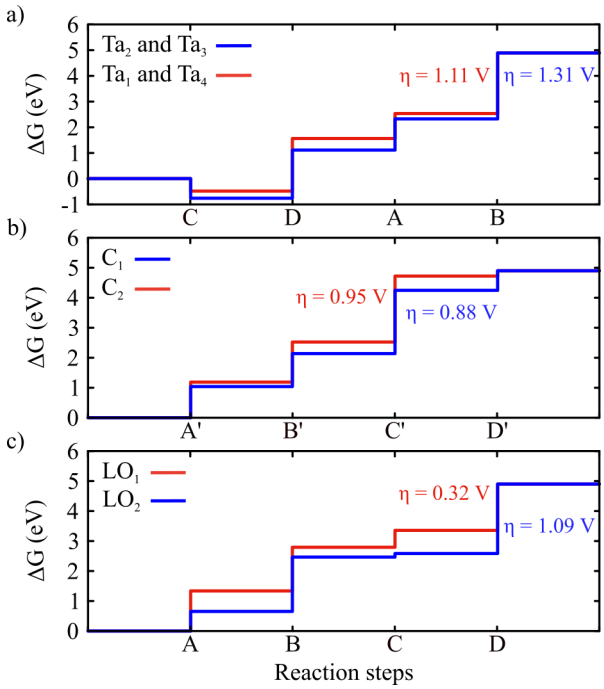

Figure S4. Free energy diagram of the OER reaction steps under operating conditions for a) the conventional mechanism, b) the coupling mechanism and c) lattice oxygen mechanism

We performed a climbing-image NEB calculation for the coupling mechanism C_3 of two oxygen adsorbates. As shown in figure S5, there is only a small barrier of 0.31 eV before the large decrease in energy associated with the O_2 formation and its desorption.

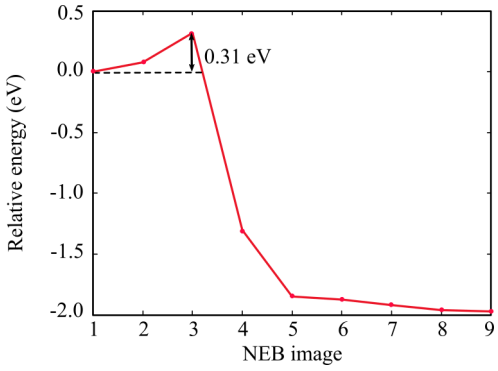

Figure S5. The energy barrier of the coupling mechanism C_3 at the reconstructed (001) surface